Progress In Electromagnetics Research B, Vol. 45, 19–35, 2012

DESIGN CONSIDERATIONS FOR RADIO FREQUENCY ENERGY HARVESTING DEVICES

D. Pavone[1, 3], A. Buonanno[2], M. D'Urso[2, *], and F. D. Corte[3]

[1]Consorzion per le Tecnologie Optoelettroniche delll'InP c/o SELEX Sistemi Integrati S.p.A., Engineering Directorate, Via Circumvallazione Esterna di Napoli, zona ASI, Loc. Pontericci, Giugliano, Napoli I-80014, Italy

[2]SELEX Sistemi Integrati S.p.A., Engineering Directorate, Via Circumvallazione Esterna di Napoli, zona ASI, Loc. Pontericci, Giugliano, Napoli I-80014, Italy

[3]DIMET, Mediterranea University of Reggio Calabria, Via Graziella-Feo di Vito, RC 89100, Italy

Abstract—Radio Frequency Energy harvesting is a research topic of increasing interest, related to sustainability, which could become a promising alternative to existing energy resources. The paper will show all the activities addressed to design a wideband system to recover wideband energy from electromagnetic sources present in the environment. The main idea is to develop battery-free wireless sensors able to capture the available energy into the mentioned bandwidth. The final goal is to realize self-powered Wireless Networks based on Ultra Lower Power — ULP sensors minimizing the need of dedicated batteries. This last feature is particularly attractive in different kind of applications, ranging from military to civil cases. A first system prototype is shown and discussed. Conclusion follows.

1. INTRODUCTION AND MOTIVATIONS

In recent years there has been an increasing interest in the development of Wireless Sensor Networks (WSNs). These networks can be uses in different scenarios as intelligent office spaces, medical monitoring and military applications. A WSN is characterized by low bit-rates, volume

Received 29 June 2012, Accepted 15 October 2012, Scheduled 19 October 2012

* Corresponding author: Michele D'Urso (mdurso@selex-si.com).

constraints for the nodes and hundreds microwatts power consumption. The use of primary batteries limits the sensor lifetime. The low power requirement of the network sensor node and the need of eliminating primary batteries pushes toward the possibility of powering the nodes by scavenging ambient power from the surroundings [1, 2]. This can potentially extend the lifetime of a node to infinite duration of time and reduce the maintenance costs associated with battery-operated devices.

The applications for these WSN normally require an operating distance of 3 to 100 meters and they usually have a backup battery in case the power provided by the RF radiation is insufficient. Other applications for RF powered devices include access control, equipment monitoring and even personal identification. In all of these applications, there must be a power conversion circuit that can extract enough DC power from the incident electromagnetic waves for the passive device to operate. In a far field RF energy harvesting system, RF energy must be extracted from the air at very low power density since the propagation energy drops off rapidly as distance from the source is increased. In free space, the electric field and power density drop off at the rate of, where is the distance from the radiating source. The available power to the receiver decreases by 6 dB for every doubling of distance from the transmitter.

In the following tables, are indicated the main electromagnetic sources and the relative power density available in the input RF energy harvesting architecture (before the conversion to DC) for outdoor-indoor applications.

The paper wants to define the design guidelines of such systems to optimize the overall performances. Note the amount of energy to harvest can be limited in the problem at hand: note that the Italian law DPCM of 8 July 2003, for example, fixes the limit values of the electromagnetic radiations to $1\,\mathrm{W/m^2}$ between 3 MHz and 3 GHz [3], thus reducing the energy available in the environment. Of course, the use of wideband architectures can overcome such limitations, thus maximizing the harvested energy.

For these reasons wideband system architecture based on

Table 1. Density power available for the 50 kW AM radio station.

50 kW AM RADIO STATION	
DISTANCE	DENSITY POWER AVAILABLE
5 km	$159\,\mu\mathrm{W/m^2}$
10 km	$40\,\mu\mathrm{W/m^2}$

Table 2. Density power values available for the 100 W GSM base station.

100 W GSM BASE STATION	
DISTANCE	DENSITY POWER AVAILABLE
100 m	800 $\mu W/m^2$
500 m	32 $\mu W/m^2$
1000 m	8 $\mu W/m^2$

Table 3. Density power available for the 0.5 W mobile phone.

0.5 W MOBILE PHONE	
DISTANCE	DENSITY POWER AVAILABLE
1 m	40 mW/m^2
5 m	1.6 mW/m^2
10 m	0.4 mW/m^2

Table 4. Density power available for the 1 W Wi-Fi router.

1 W Wi-Fi ROUTER	
DISTANCE	DENSITY POWER AVAILABLE
1 m	80 mW/m^2
5 m	3.2 mW/m^2
10 m	0.8 mW/m^2

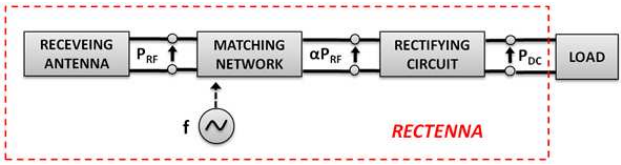

Figure 1. Energy harvesting architecture.

radiofrequency energy harvesting, able to recover energy from available RF electromagnetic sources to power wireless sensor nodes is presented.

The paper is organized as follows. In Section 2 the overall problem is introduced. Section 3 and Section 4 deal with the design, simulation, realization and characterization of a first prototype working at 900 MHz. In Section 4, the multiband solution is proposed and realized. Section 5 concerns possible application to batteries-free sensor networks.

2. OVERALL SYSTEM ARCHITECTURE

The basic structure of an energy harvesting system is shown in Fig. 1 [4]. The front-end is the receiving antenna. It converts the input microwave signal into AC voltages and currents. The matching

network between the receiver antenna and rectifier circuit is necessary to further reduce the transmission loss (high matching efficiency α with $0 \leq \alpha \leq 1$) and to increase the input voltage of the rectifier circuit. The output voltage of the matching network is AC type, but the electronic loads require DC voltage for their operation. Therefore, the AC voltage of the output has to be processed by a suitable power converter to produce the required DC voltage for the load. The device assigned to this aim is the rectifying circuit.

3. SINGLE FREQUENCY ENERGY HARVESTING ARCHITECTURE

To obtain an effective energy harvesting system, the rectenna must exhibit high RF-DC conversion efficiency η defined as:

$$\eta = \frac{P_{\mathrm{DC}}}{P_{\mathrm{RF}}} \times 100[\%] = \frac{V_{\mathrm{DC}out}^2/R_L}{P_{\mathrm{RF}}} \times 100[\%] \tag{1}$$

where the P_{DC} is the output DC power harvested, P_{RF} the input RF power and R_L is the load to supply (see Fig. 1). The diode is the main part of the rectifying circuit; it changes the AC microwave signal into DC signal. A diode with a lower built-in voltage would realize a higher rectifying efficiency. Due to its nonlinear characteristics, the diode will create harmonic signals, which can notably decrease the rectifying efficiency of the system [5]. Moreover, this spurious harmonics could to modify the typical working of the load. An effective design of the above mentioned RF energy harvesting system cannot neglect these issues. In the following, the design guidelines for the rectifying circuit and the matching network are addressed.

3.1. Rectifying Circuit

Different ways to rectify AC signals have been introduced in [6]. In [6], the *voltage doubler rectifier (VDR) has been exploited*. The latter exhibits two main interesting features matching the addressed RF energy harvesting application. The first one concerns the capability to enhance the low RF input voltage; the second one is related to the ability of working without external bias supply. The VDR circuit has shown in Fig. 2. It consists of a peak rectifier formed by D1 and C2 and a voltage clamp formed by D2 and C1. The VDR output is:

$$V_{OUT=}\left(2V_{\mathrm{RF}amp} - V_{th1} - V_{th2}\right) \tag{2}$$

where V_{th} is the threshold voltage of the diode and $V_{\mathrm{RF}amp}$ is the RF input voltage. The individual stages of VDR circuit can be arranged in

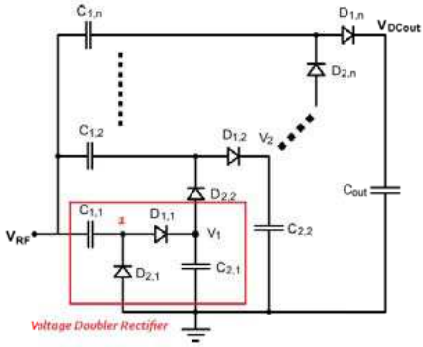

Figure 2. N-stage voltage multiplier as the cascade of the N-VDR.

cascade as reported in Fig. 2 (N-stage voltage multiplier) to increase the output voltage of the rectifier [7].

$$V_{OUT=}\left(2NV_{\mathrm{RF}amp}-2NV_{th}-\frac{(N-1)I_{LOAD}}{f_0*C}\right) \tag{3}$$

where I_{LOAD} is the load current, C are the blocking capacitor and f_0 is the working frequency.

When the rectifier stages are cascaded, each rectifier stage acts as a passive voltage level shifter in addition to the voltage shift in voltage clamp and peak rectification. To better explain such a point, let suppose that a sinusoidal voltage, say V_{RF}, with a frequency f_0 and amplitude $V_{\mathrm{RF}amp}$, is applied as input of the voltage multiplier. To assure a small ripple in the output voltage, capacitances have to be dimensioned so that their time constant is much smaller than the period of the input signal, that is, $1/(2\pi CR_L) \ll f_0$, C being the blocking capacitors and R_L the equivalent load resistance. The average input power, P_{IN} required to obtain a given output voltage and power can be evaluated by summing up the average power, P_D, dissipated in each diode and the power, P_L, transferred to the load. By increasing the number of stages N (or equivalently the number of diodes) the value of average dissipated power P_D increases. Taking into account substrate losses, the average input power is given by,

$$\begin{aligned} P_{IN} &= 2NI_{D,SAT}B_1\left(\frac{V_{OUT}}{V_T}\right)\exp\left(-\frac{V_{\mathrm{RF}amp}}{2NV_T}\right) \\ &\quad +\frac{N}{2}V_{OUT}^2R_{SUB}\left(\omega_0C_{SUB}\right)^2 \end{aligned} \tag{4}$$

where V_T, is the thermal voltage and B_1 is the modified Bessel function of order one and R_{SUB} and C_{SUB} are the substrate resistance and

capacitance, respectively [8]. Solving (4) by numerical iteration, for a fixed output voltage and power consumption, it is possible to note that higher is the number of stages smaller is the amplitude of the input voltage required to obtain a given DC output voltage and power consumption. However, optimal number of stages should be found with a compromise between high DC output voltage and low power loss due to power consumption of diodes and the loss of the substrate. The tests have shown that the optimum number N of stages is between 1 and 2. To reduce the loss in the diode, the diode should have large saturation current $I_{D,SAT}$, low junction capacitance C_J which result in low threshold voltage V_{th}, small series resistance Rs and small junction resistance R_J [9]. The AVAGO HSMS family diodes represent a good market solution for these applications.

3.2. Power Matching

The equivalent input impedance of the voltage multiplier can be represented, as a zero-order approximation, by the parallel of a resistance and capacitance [8]. In the high frequency analysis of the voltage multiplier, the input capacitance is the parallel of all the diodes capacitances while the equivalent input resistance, R_{in_eq}, is the resistance calculated from power consumption as

$$R_{in\_eq} = \frac{V_{\mathrm{RF}amp}}{2P_{IN}} \tag{5}$$

In order to obtain a good matching between the RF source and voltage multiplier, assigned the DC load in terms of voltage V_{OUT} and power P_{OUT}, the first step is to calculate the voltage $\mathrm{V_{RF}}amp$ (RF input voltage to the voltage multiplier) in order to obtain the V_{OUT} and the P_{OUT}. Performing a sweep of the RF input power, it is possible calculate the input impedance in terms of equivalent input resistance and capacitance. Fixed the voltage V_{OUT} and power P_{OUT}, in order to compensate the equivalent input capacitance of the voltage multiplier, a proper inductance L', in parallel with the input of the voltage multiplier, can be introduced. In this way, the input impedance of voltage multiplier can be schematized as a resistive load. Again, performing a sweep of the RF input power and fixed the output power P_{OUT}, it is possible to calculate the input resistance, R_{in_eq} (5) and consequently the voltage $V_{\mathrm{RF}amp}$. In this way, by an impedance transformer LC (classic $\lambda/4$ transformer with L referred to ground) it is possible calculate the input voltage VIN_RF of it that correspond at the output voltage antenna.

To realize the $\lambda/4$ transformer, a discrete LC matching network circuit has been used, thus achieving a voltage gain (between VIN_RF

and $V_{\mathrm{RF}amp}$) of a Q-factor [5] defined as

$$Q = \sqrt{\left(\frac{R_{in\_eq}}{R_{ANT}}\right) - 1} \tag{6}$$

where R_{ANT} is the antenna resistance.

Input capacitance due to the diodes is variable with the voltage across diodes, L' is chosen in order to resonate with its average value at the operating frequency f_0. This leads to the condition,

$$\Delta C \ll \frac{Q}{2\pi f_0 R_{in\_eq}} \tag{7}$$

where ΔC is the maximum variation of the input capacitance of the voltage multiplier with respect to its mean value.

Note the matching circuit is a key element of the harvesting system. Indeed, the conversion efficiency of the system η [see (1)] is closely related to the impedance matching between the antenna and the rectifier circuit that is a nonlinear function of both power input and frequency.

In particular, the matching network LC is a resonator circuit (non-linear) working at the designed frequency according to the diodes rectifier. Of course, the conversion efficiency η is high at the designed frequency and extremely low elsewhere.

With regards to the input power, as the R_{in_eq} and V_{out} of the VDR is a non linear function with the power input (see (4)), the Q-factor of the matching network changes and accordingly the conversion efficiency η. In order to obtain good conversion efficiency η, it is useful to design the matching network around a specific power input (considering the losses of the circuit, it must be higher than output power P_{OUT}) because it is possible supposed that the circuit works in conditions of linearity about it. Small shifts around this power (more less $\pm$ 5 dBm) involves a good parameter η, conversely it drops quickly. This explains why the characteristic efficiency curve presents a bell-shaped.

4. SINGLE FREQUENCY PROTOTYPE

In the following, according to the guidelines, an interesting and very compact rectenna working at 900 MHz is designed, realized and characterized. The RF/DC converter is a 2-stage voltage rectifier. It has been designed and simulated by using the Advanced Design System (ADS) software, which properly uses the Harmonic-Balance (HB) method. For the circuit realization, it has been used the commercial zero biased Schottky diode HSMS2850, 1 nF blocking

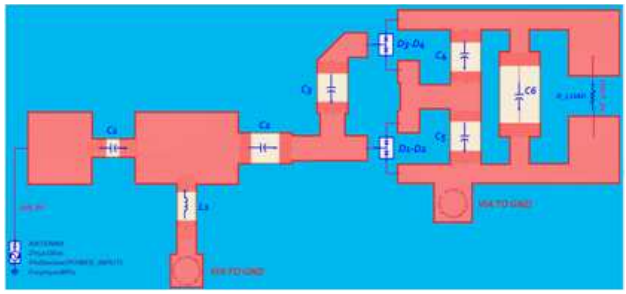

Figure 3. EM/circuit co-simulation setup at 900 MHz.

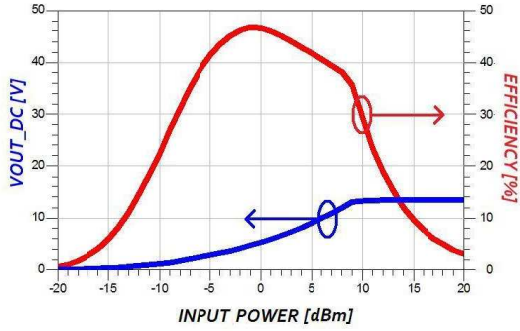

Figure 4. Co-simulation results: output voltage and efficiency rectification of the 900 MHz rectenna varying the RF input power.

capacitors and 100 nF output capacitor (Fig. 3). A 60 kΩ load, approximating an ultra-low power sensor, has been considered. The matching circuit has been designed according to guidelines in Section 3. To obtain very compact size a concentrated parameter implementation of the matching circuit has been adopted. In order to obtain very accurate numerical results, it has been co-simulated the rectifier with momentum ADS including diode models and capacitor and inductor packaging (Fig. 3).

Performing a sweep of the RF input power (between −20 dBm and 20 dBm), it is possible to plot the DC output voltage and the efficiency rectification RF-DC of the circuit simulated with real component (accounting of the substrate loss) (Fig. 4).

As it can be seen, the designed system exhibits a very high efficiency, due to the effective guidelines previously derived. Notably, the realized system is characterized by an improved efficiency with respect to the ones reported in [10, 11].

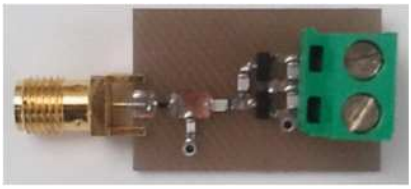

Figure 5. Single frequency prototype rectenna.

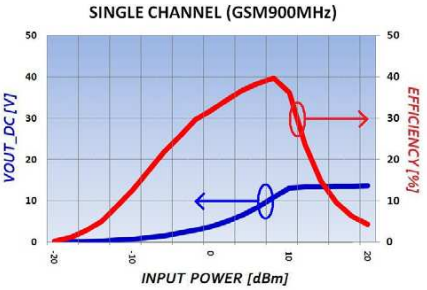

Figure 6. Measurements: output voltage and efficiency rectification of the 900 MHz rectenna varying the RF input power.

4.1. Experiments Results

As simple prototype is shown in Fig. 5. The layout size of the harvesting system is 2.1 cm × 1 cm. It has been fabricated using 0.5-oz copper (0.017 mm thick), Rogers Duriod 5880 board material at SELEX Sistemi Integrati S.p.A. facilities available at SELEX SIstemi Integrati Giugliano site.

The overall performances have been evaluated by measuring the DC output voltage and the overall efficiency by increasing the input power of an *HP Signal Generator* from −20 dBm to 20 dBm at 900 MHz. The results are shown in Fig. 6.

The measured efficiency values, reported in Fig. 6 are slightly lower than the simulated ones (see Fig. 6), according to the fact that lumped parasitic components and the tolerances (±10%) of the capacitors and the inductor have not been considered. As highlighted in the previous section, a variation of these values involves a variation of the Q-parameter and then the variation of the conversion efficiency η. In particular, the critical component is the inductor L1 that must also to delete the capacitance input impedance of the VDR. In order to overcome this drawback, a solution could be the proper realization of the distributed matching circuit rather than discrete components.

5. MULTIBAND ENERGY HARVESTING ARCHITECTURE

This Section concerns the case of wideband energy harvesting systems. The problem comes out from the circumstance that, often, a single rectenna is not sufficient to supply the common device operations: the

problem of wideband energy harvesting systems arises, and possible solutions could be represented by a multi-antenna system [12]. In this case, each antenna (operating at different frequencies) could have its own rectifier to harvest separately DC power [13]. This configuration is suitable when multi frequency sources are available. The drawback of this configuration [13] is the need to use many antennas, thus increasing the overall costs, weight and size of the harvesting system. To overcome this drawback, a possible solution is to use only one Ultra Wide Band — UWB (or Multiband) antenna. In this case, the problem is to design the matching networks. To our knowledge, there is not a solution to this problem due to the non-linearity of the diodes with respect to both frequency and RF power input. In this paper, a novel architectural solution (Fig. 7) able to avoid the problem is proposed. In particular, knowing the N frequencies of RF sources, N matching networks working at different frequencies f_i are used. In this way, only one UWB antenna (or multi-band) connected with N rectifying circuits and relative matching network (Section 2) is considered. Note that the matching circuits have a double function. They allow to achieve the desired impedance matching and to filter the proper frequency content on each rectifier channel. In this way, the matching networks operating at different frequency band, consume a very low power when the RF input signal doesn't contain the correspondent frequency even if they are connected in parallel (see Fig. 7). In fact, the input impedance of the matching network (designed at frequency f_i) at the frequency f_j is very high (it is approximated to an open circuit). In this particular case, the lost power is approximately 3% of the total input power. The outputs from each rectifying circuit are connecting together by DC Combining Circuit in order to sum the harvested power.

To obtain the mentioned system it is very important to design an efficient DC combining circuit. An interesting solution is represented by the modified version of the single-stage full-wave Greinacher rectifier [11] showed in Fig. 8.

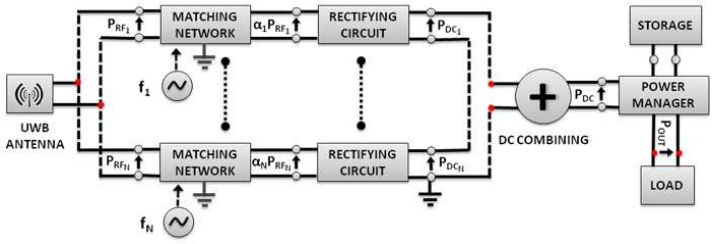

Figure 7. Multi-band energy harvesting architecture.

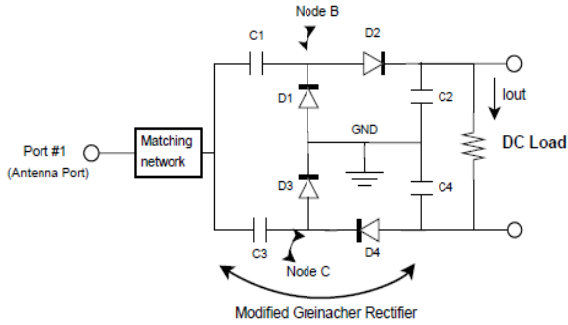

Figure 8. Schematic of the rectifier with DC combining circuit.

The modified Greinacher rectifier operates as follows. If $V_{rec}(t)$ is the induced voltage at the antenna port, then C1 and D1 shift the voltage $V_{rec}(t)$ up at node B. Subsequently, D2 and C2 rectify the voltage at node B (both RF and DC components) to appear across the DC load. Similarly, C3 and D3 shift the voltage $V_{rec}(t)$ down at node C. In turn, D4 and C4 rectify the voltage at node C to appear across the DC load. Upon reaching equilibrium, the rectifier circuit delivers a constant output current and voltage to the DC load.

In this architecture, the outputs from each rectifying circuit are properly connecting in series. This architecture allows obtaining a good rectification and DC-combining efficiency but has the disadvantage to have a differential output and a limited number of input signal ($N = 2$).

In this paper, a new solution removing these limitations has been introduced. The outputs of the N rectifier circuits have been connected in series, but the DC load is connected between the Nth rectifying circuit (referred to ground) and the first. In this way, has been extended to N the number of the RF input signals (see Fig. 7). In more detail, for every rectifier circuits (RF channel), the series of the blocking capacitors is cascaded with the previous and next RF channel while the i-th matching network is already referred to ground.

This configuration (not present in literature) allows connecting more rectifier circuits, working at different frequency, in order to harvest more energy than a single frequency circuit.

Note that, in the proposed configuration, due to the non linearity of the diode, the N output resistance of each rectifier circuit change with the input RF signals. This means that it is not possible to identify the optimum load in terms of harvested DC power. The choice of the sub-optimal load value should account of the presence and power value of RF sources.

The total harvested DC power of the proposed UWB (or multi

Table 5. Comparison between a single and multi-band energy harvesting architecture.

MULTIBAND ENERGY HARVESTING SYSTEM	
ADVANTAGES	DRAWBACKS
MORE POWER RECOVERABLE BY A MULTI-BAND ANTENNA	SAME CONVERSION EFFICIENCY
WORK FLEXIBILITY	DC COMBINING EFFICIENCY
LOW (NO ULTRA LOW) POWER LOAD	

band) energy harvesting architecture is:

$$P_{\mathrm{DC}} = e \sum_{i}^{N} G_i P_{\mathrm{RF}}^{i} \eta \tag{8}$$

where η refers to the RF to DC conversion efficiency, e denotes the efficiency of the DC combining circuit and G_i refers to antenna's gain corresponding at i-th frequency. As it can be seen from (8), by properly designing the rectifying and the DC combining circuits, is possible to sensibly increase the DC power harvested through the adoption of a larger number of RF sources and the antenna gain. In this way, the energy harvested from the multi-band energy harvesting architecture (Fig. 7) can be enough to power different kind of ULP load.

In order to manage the harvested energy, it is also mandatory to exploit a power manager device. It allows to supply sensors requiring short time high load current (low duty cycle). The power manager is also able to charge an energy storage (e.g., supercapacitor) that provides energy to the load when the input power may be lost.

Finally, in Table 5, the comparison between a single and multi-band energy harvesting architecture is showed.

5.1. Simulation

In the following, an interesting and very compact rectenna working at 900 MHz and 2.4 GHz is designed, realized and characterized. The RF/DC converters are a 2-stage voltage rectifier. For the simulations, it has been used the commercial zero biased Schottky diode HSMS2852 and HSMS2862 models respectively for the RF/DC converter at 900 MHz and 2.4 GHz (Fig. 9). A 60 kΩ load, approximating an ultra-low power sensor, has been considered. The matching circuit has been designed according to guidelines in Section 3. To obtain very compact

size a concentrated parameter implementation of the matching circuit has been adopted.

As before, performing a sweep of the two RF inputs power between −20 dBm and 20 dBm (the power is the same for each RF source), it is possible to plot the DC output voltage and the efficiency rectification RF-DC of the circuit simulated with real component (Fig. 10).

As it can be seen, the designed system exhibits a very high efficiency, due to the effective guidelines previously derived.

Let analyze the efficiency rectification of the proposed architecture

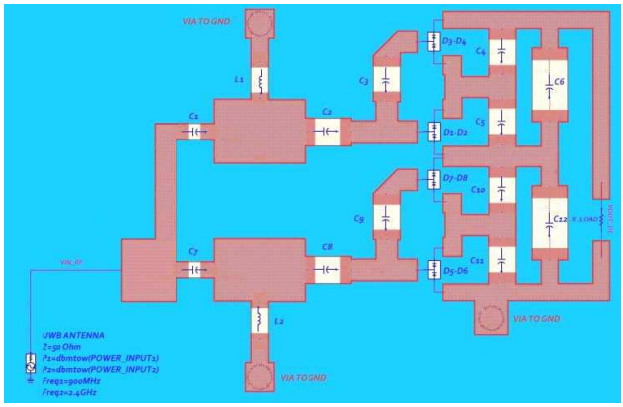

Figure 9. EM/circuit co-simulation setup at 900 MHz and 2.4 GHz.

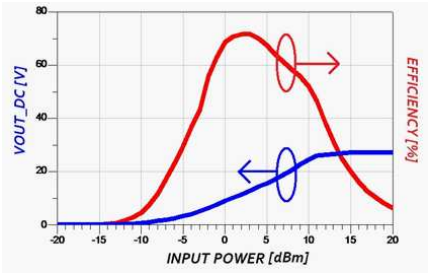

Figure 10. Co-simulation results: output voltage and efficiency rectification of the 900 MHz–2.4 GHz rectenna varying the RF input power.

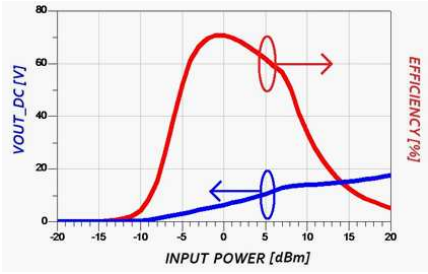

Figure 11. Co-simulation results: output voltage and efficiency rectification of the 900 MHz–2.4 GHz rectenna varying the RF input power 1 (900 MHz) while, the RF input power 2 (2.4 GHz) is −30 dBm.

in some special cases varying the power of one of the two RF sources. In particular, the Fig. 11, shows the case when the input power at 2.4 GHz is very low (−30 dBm) while the input power at 900 MHz vary between −20 dBm and 20 dBm. Reversed case is showed in Fig. 12.

The simulations show a very good efficiency conversion for both the shown cases.

5.2. Experiments Results

In order to demonstrate the validity of the broadband architecture, it has been realize the layout of the circuit shown in Fig. 9. The antenna considered has been the directional four band panel antenna suitable for simultaneous GSM-DCS-UMTS-Wireless application in the 900/1800/2200/2500 MHz bands. The RF sources (at 900 MHz and 2.4 GHz) used are mentioned respectively in Tables 3 and 4. The distance between the two sources and the antenna was about 1 m.

Before to show the achieved result, in order to evaluate the soundness of the developed guide lines, the numerical simulation of the considered scene is considered.

In particular, compatible with the values of Tables 3 and 4, the RF input power1 (900 MHz) is 4.5 dBm (2.8 mW) and the RF input power 2 (2.4 GHz) is 1.7 dBm (1.5 mW).

In this case is obtained the rectification efficiency of about 75% with total DC output power of about 3 mW (4.7 dBm) and the DC output voltage of about 13 V (see Fig. 13).

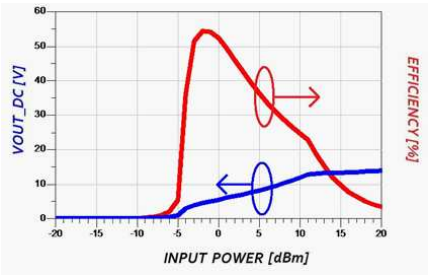

Figure 12. Co-simulation results: output voltage and efficiency rectification of the 900 MHz–2.4 GHz rectenna varying the RF input power 2 (2.4 GHz) while, the RF input power 1 (900 MHz) is −30 dBm.

Figure 13. Co-simulation results: output voltage and efficiency rectification of the 900 MHz–2.4 GHz rectenna when the RF input power1 (900 MHz) is 4.5 dBm and the RF input power 2 (2.4 GHz) is 1.7 dBm.

The calculation of the power input has been made, considering the antenna's gain and the distance between RF sources and receiving antenna.

The described experimental setup is shown in Fig. 14. In this experiment an output voltage of 12.2 V on a load of 60 kohm has been measured. More in detail, the output power (2.48 mW) is slightly lower than that simulated (3 mW) due to the numerical model approximation and the not exact knowledge of the input parameters.

This means that the designed system works correctly and in line with the required performances.

6. APPLICATION TO BATTERIES-FREE SENSOR NETWORKS

The developed architectures have the aim to make any sensor batteries-free. In particular, in this section, the eZ430-RF2500 sensor has been powered with the single frequency prototype rectenna shows in Fig. 5 without the use of batteries. This last feature is particularly attractive in different kind of applications, ranging from military to civil cases.

The eZ430-RF2500 is a complete USB-based MSP430 wireless development tool providing a 2.4-GHz wireless transceiver. It is preloaded with a reprogrammable wireless temperature sensor. The considered network consists of an *Access Point* that measures its own temperature and also wirelessly receives temperature measurements from *End Devices (ED)*. End Devices measure their temperature once per second and then enter a low-power mode to reduce battery usage. The average current calculation must also take into account

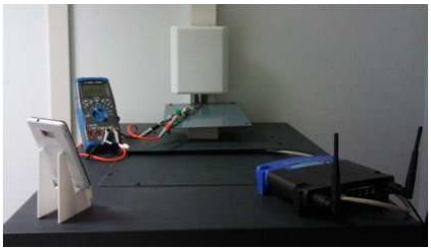

Figure 14. Multiband energy harvesting experimental.

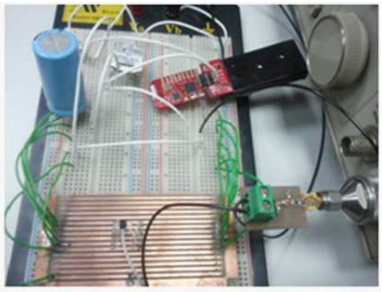

Figure 15. The overall harvesting system including LTC3108, eZ430-RF2500 and supercapacitor.

the sleep current of the ED. The average current consumption for the considered application is 36.80 μA (for one second of the transmission period). Typically, the eZ430-RF2500 sensor is supplied by two 1.5 volts alkaline batteries. The average power consummation of the sensor node is roughly 100 μW (−10 dBm) corresponding to our measured value using −4 dBm input RF power at 900 MHz (see Fig. 6). This proves that having a low power RF source (less than a typical cell phone output radiated power) is possible to self-power the considered ULP temperature sensor node. The overall realized harvesting system including the LTC3108 power management, a supercapacitor and the sensor node as shown in Fig. 15.

Of course, we expect that the use of the multi-band architecture can improve the performances.

7. CONCLUSIONS

This paper presents the design criteria for the multi-band RF energy harvesting system. In particular the design tradeoffs of each block of the proposed multi-band architecture have been derived and discussed. Two systems enable to harvest RF power at 900 MHz GSM band (single frequency) and at 900 MHz GSM–2.4 GHz Wi-Fi bands (multi-frequency) have been designed and realized.

The prototype a single frequency (900 MHz) has been used to supply eZ430-RF2500 wireless sensor node. In particular, at −4 dBm input power, the system recovers 160 μW with 3 V DC output (32% RF-DC rectification efficiency). It has been shown that the generated DC power is sufficient to power sensor nodes (eZ430-RF2500). Two aspects have to be underline. Firstly, the obtained results show the proposed harvesting system is able to recover the available RF energy by using opportunity sources and to supply ULP wireless sensor nodes. Second, the proposed system could represent, on a large scale, a suitable solution to environmental sustainability: it allows reducing the use of batteries, sources of environmental pollution.

REFERENCES

1. Warneke, B. A., "An autonomous 16 mm^3 solar-powered node for distributed wireless sensor networks," *Proc. of IEEE Sensors*, Vol. 2, 1510–1515, Jun. 12–14, 2002.
2. Meninger, S., J. O. Mur-Miranda, R. Amirtharajah, A. Chandrakasan, and J. H. Lang, "Vibration-to-electric energy conversion," *IEEE Trans. on VLSI Systems*, Vol. 9, No. 1, 64–76, Feb. 2001.

3. Decree of President of the Council of Ministers, Jul. 8, 2003.
4. Zhu, N., K. Chang, M. Tuo, P. Jin, H. Xin, and R. W. Ziolkowski, "Design of a high-efficiency rectenna for 1.575 GHz wireless low power transmission," Department of Electrical and Computer Engineering, University of Arizona, Tucson, Arizona, USA, 2011.
5. Akkermans, J. A. G., M. C. van Beurden, G. J. N. Doodeman, and H. J. Visser, "Analytical models for low-power rectenna design," *IEEE Antennas and Wireless Propagation Letters*, Vol. 4, 2005.
6. Razavi, B., *RF Microelectronics*, Prentice Hall PTR, 1997.
7. Karthaus, U. and M. Fischer, "Fully integrated passive UHF RFID transponder IC with 16.7-μm minimum RF input power," *IEEE Journal of Solid-State Circuits*, Vol. 38, 1602–1608, Oct. 2003.
8. De Vita, A. and G. lannaccone, "Design criteria for the RF section of long range passive RFID systems," *Proc. Norchip Conference,* 107–110, Oslo, Norway, 2004.
9. Buted, R. R., "Zero bias detector diodes for the RF/ID market," *Hewlett-Packard Journal*, Dec. 2005.
10. Yan, H., M. Popadic, J. C. Macias, L. C. N. de Vreede, A. Akhnoukh, and L. K. Nanver, "Design of an RF power Harvester in a silicon-on-glass technology," *Proc. of 19th Annual Workshop on Circuits, Systems and Signal Processing*, 287–290, Ultrcht, 2008.
11. Wilas, J., K. Jirasereeamornkul, and P. Kumhom, "Power harvester design for semi-passive UHF RFID tag using a tunable impedance transformation," *Proc. of the IEEE Conference ISCIT*, 1441–1445, Sep. 2009,
12. Olgun, U., C. C. Chen, and J. L. Volakis, "Investigation of rectenna array configurations for enhanced RF power harvesting," *IEEE Antennas and Wireless Propagation Letters*, Vol. 10, 2011.
13. Hagerty, J. A., F. B. Helmbrecht, W. H. McCalpin, R. Zane, and Z. B. Popovic, "Recycling ambient microwave energy with broadband rectenna arrays," *IEEE Trans. on Microwave Theory and Techniques*, Vol. 52, No. 3, Mar. 2004.